

## Determination of Disulfide Bond Connectivity of Cysteine-rich Peptide IpTx<sub>a</sub>

Chul Won Lee,<sup>\*</sup> Kazuki Sato,<sup>†</sup> and Jae Il Kim<sup>\*,‡</sup>

Department of Chemistry, Chonnam National University, Gwangju 500-757, Korea. \*E-mail: cwlee@jnu.ac.kr

<sup>†</sup>Fukuoka Women's University, Kasumigaoka, Higashi-ku, Fukuoka 813-8529, Japan

<sup>‡</sup>Department of Life Science, Gwangju Institute of Science and Technology (GIST), Gwangju 500-712, Korea

\*E-mail: jikim@gist.ac.kr

Received March 4, 2013, Accepted March 20, 2013

**Key Words :** Cysteine-rich peptide, Disulfide bond, Imperatoxin A, Ion channel, Ryanodine receptor

Disulfide bonds play a crucial role in the folding and structural stabilization of many important extracellular peptides and proteins including hormones, enzymes, growth factors, toxins, and immunoglobulins.<sup>1,2</sup> Cysteine-rich peptides stabilized by intramolecular disulfide bonds have often been isolated from venoms of microbes, animals and plants. These peptides typically have much higher stability and improved biopharmaceutical properties compared to their linear counterparts. Therefore the correct disulfide bond formation of small proteins and peptides has been extensively studied for a better understanding of their folding mechanism and achieving efficient generation of the naturally occurring biologically active product. Imperatoxin A (IpTx<sub>a</sub>), a peptide toxin containing 6 cysteine residues, was isolated from the venom of scorpion *Pandinus imperator*, selectively binds the ryanodine receptors and activates Ca<sup>2+</sup> release from sarcoplasmic reticulum (SR).<sup>3,4</sup> IpTx<sub>a</sub> increases the binding of ryanodine to ryanodine receptors (RyRs)<sup>4,5</sup> and encourages reconstituted single channel to induce subconductance states.<sup>5</sup> We previously reported the three-dimensional structure of IpTx<sub>a</sub> determined by solution NMR spectroscopy.<sup>6</sup> The molecular structure of IpTx<sub>a</sub> consists of two antiparallel  $\beta$ -strands connected by four chain reversals. The overall structure of IpTx<sub>a</sub> is stabilized by three disulfide bonds. This topology and disulfide bond pattern is classified as an 'inhibitor cysteine knot' fold found in numerous toxic and inhibitory peptides,<sup>7-11</sup> including  $\omega$ -conotoxins. Figure 1 shows the sequence alignment of IpTx<sub>a</sub> with  $\omega$ -conotoxin GVIA, MVIIA, and MVIIC demonstrating the same number and position of cysteines, although they have very low Dali Z-scores and sequence identity. IpTx<sub>a</sub> exhibits a large functional surface area identified by alanine-scanning mutagenesis, and the hydrophobic core of IpTx<sub>a</sub> is entirely composed of the four out of six cysteines that form intramolecular disulfide bonds to stabilize the overall toxin structure. Without cysteine residues, IpTx<sub>a</sub> completely lost its molecular structure and biological activity.<sup>6</sup> These results indicate that the information of the authentic disulfide bond connectivity of cysteine-rich peptides or proteins might help not only to understand their three-dimensional conformation but to prepare biologically active products. Here we report the disulfide bond connectivity of IpTx<sub>a</sub> determined by a combined approach of enzymatic fragmentation and chemical synthesis. The disulfide

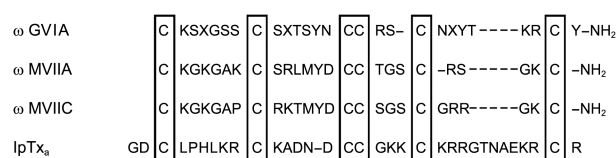


**Figure 1.** Primary sequences of  $\omega$ -conotoxin GVIA, MVIIA, MVIIC, and IpTx<sub>a</sub> (X=Hyp).

bond connectivity of IpTx<sub>a</sub> is the same as that of  $\omega$ -conotoxins (between the 1<sup>st</sup> and 4<sup>th</sup>, 2<sup>nd</sup> and 5<sup>th</sup>, and 3<sup>rd</sup> and 6<sup>th</sup> cysteines). The role of disulfide bonds of IpTx<sub>a</sub> is discussed.

### Experimental

**Peptide Synthesis and Oxidative Folding.** Solid phase peptide synthesis was conducted on an Applied Biosystems 433A peptide synthesizer. The linear precursor of IpTx<sub>a</sub> was synthesized by solid phase methodology of Fmoc chemistry starting from Fmoc-Arg(Pmc)-Alko resin using a variety of blocking groups for the protection of amino acids. MALDI-TOF-MS was measured on a PerSeptive Biosystems Voyager Linear mass spectrometer by using  $\alpha$ -cyano-4-hydroxy-cinnamic acid as a matrix. High performance liquid chromatography (HPLC) analysis was performed on a Shimadzu LC-6AD system and Shimadzu LC-10Avp system with ODS column (4.6  $\times$  250 mm). Preparative HPLC was performed with a Shimadzu LC-6AD system and Shimadzu LC-10Avp system with ODS column (20  $\times$  250 mm). The linear precursor of IpTx<sub>a</sub> assembled by Fmoc solid-phase synthesis were cleaved from the resin with a mixture of TFA (trifluoroacetic acid), H<sub>2</sub>O, ethanedithiol, phenol, and thioanisole (percentage volume ratios 82.5/5/2.5/7.5/5). After being stirred for 3 h at room temperature, the solution was cooled and mixed with a 10-fold volume of diethyl ether precooled at 0 °C. The resultant precipitates were collected on a glass filter and washed thoroughly with dimethyl ether. The deprotected peptides were extracted from the resin with 2 M acetic acid. The deprotected linear peptides were diluted to a final peptide concentration of 2.5  $\times$  10<sup>-5</sup> M and subjected to oxidative disulfide bond formation at 4 °C for 3 days in 0.1 M ammonium acetate buffer (pH 7.8) containing 0.1 M NaCl, 20 mM Na<sub>2</sub>HPO<sub>4</sub>, and reduced/oxidized glutathione finally 2.5 mM and 0.25 mM, respectively. When close to

equilibrium, the reactions were stopped by lowering the pH  $\sim 4$  with acetic acid. The acidified solutions were filtered through paper and 0.22  $\mu\text{m}$  membrane filters, and then loaded onto an ODS column [(30  $\times$  50 mm) + (20  $\times$  250 mm)] by a medium pressure pump. After nonadsorbed components had been washed out, the peptides were eluted with 50% acetonitrile containing 0.1% TFA.

**Purification of Folded IpTx<sub>a</sub>.** The crude peptides were dissolved in 5–10 mL of 0.01 M NH<sub>4</sub>OAc buffer (pH 4.5) and applied to a column (18  $\times$  200 mm) of CM-cellulose CM52 equilibrated with 0.01 M NH<sub>4</sub>OAc buffer (pH 4.5). Peptides were eluted at a flow rate of 15 mL/12 min with a linear gradient of 500 mL of 0.01 M NH<sub>4</sub>OAc buffer (pH 4.5) and 500 mL of 0.7–0.9 M NH<sub>4</sub>OAc buffer (pH 6.5). The fractions containing IpTx<sub>a</sub> were lyophilized and injected into an ODS (C18, 20  $\times$  250 mm) HPLC column. IpTx<sub>a</sub> was eluted with a linear gradient of 10%–20% acetonitrile in 0.1% TFA for 20 min. The purity and molecular weight of the synthetic peptide were confirmed by analytical HPLC and MALDI-TOF-MS measurements.

**Determination of Disulfide Bond Connectivity of IpTx<sub>a</sub>.** IpTx<sub>a</sub> was digested with lysyl endopeptidase in 0.1 M phosphate buffer (pH 6.5) at 37  $^{\circ}\text{C}$  for 5 h. Enzymatic fragments were isolated and analyzed by RP-HPLC and MALDI-TOF-MS measurements. Two authentic peptides containing two disulfide bridges were synthesized by the method previously reported<sup>12,13</sup> with some modifications. Two peptides having two free thiol groups and one Ac<sub>m</sub>-protected thiol group were synthesized by Fmoc chemistry. The first disulfide bond was formed in 0.2 M ammonium acetate buffer at pH 7.8. The resulting product was then made to react with 3-nitro-2-pyridinesulfonyl chloride (Npys-Cl) in acetic acid at room temperature for 20 minutes to convert the Ac<sub>m</sub> group into the Npys group. The Cys(Npys)-containing peptide thus obtained was purified by RP-HPLC and then mixed with

two equimolar amount of Arg-Cys-Arg peptide in 1 M acetic acid for 39 h at room temperature to form the second disulfide bond. The bicyclic peptide was cleaved by lysyl endopeptidase. The product was compared with enzymatic fragment on RP-HPLC.

**CD Measurement.** CD spectra were measured on a JASCO J-715 spectropolarimeter in H<sub>2</sub>O solution (0.01 M sodium phosphate, pH 7.0) at 20  $^{\circ}\text{C}$  at the concentrations of 0.05 mM for 190–250 nm and 1 mM for 240–360 nm by using a quartz cell of 1 mm path length. The spectra were obtained as an average of 4 scans at a scan speed of 20–50 nm/min, with a sensitivity range of 20 mdeg/FS, using an instrumental time constant of 1 s. The spectra are expressed as molecular ellipticity [ $\theta$ ] in degree  $\text{cm}^2 \text{dmol}^{-1}$ .

## Results and Discussion

Synthesis of the linear peptide proceeded smoothly, as indicated by monitoring of the Fmoc deprotection peak at each cycle. Figure 2 shows the HPLC profiles from TFA cleavage to final purification of IpTx<sub>a</sub>. After TFA cleavage, the linear precursor of IpTx<sub>a</sub> from which all the protective groups had been removed was extracted from the resin with 2 M acetic acid. Air oxidation of the crude linear peptide afforded peptide having proper disulfide bond pairings as the major products, which was purified by ion exchange chromatography and HPLC. The folded peptide was obtained in good isolation yield (4% from the starting resin). Since IpTx<sub>a</sub> is a very basic peptide with net charge = +8 at neutral pH, we used CM-cellulose CM52 as a cation exchange chromatography using NH<sub>4</sub>OAc buffer gradient as eluent. The final purified IpTx<sub>a</sub> were confirmed by analytical HPLC and MALDI-TOF-MS measurements.

To determine the disulfide bond structure of IpTx<sub>a</sub>, we used enzyme fragmentation and peptide chemical synthesis. The purified IpTx<sub>a</sub> was digested with lysyl endopeptidase and analyzed by RP-HPLC and MALDI-TOF-MS measurements (Figure 3). The most intense peak on the RP-HPLC was derived from fragment containing two disulfide bonds.

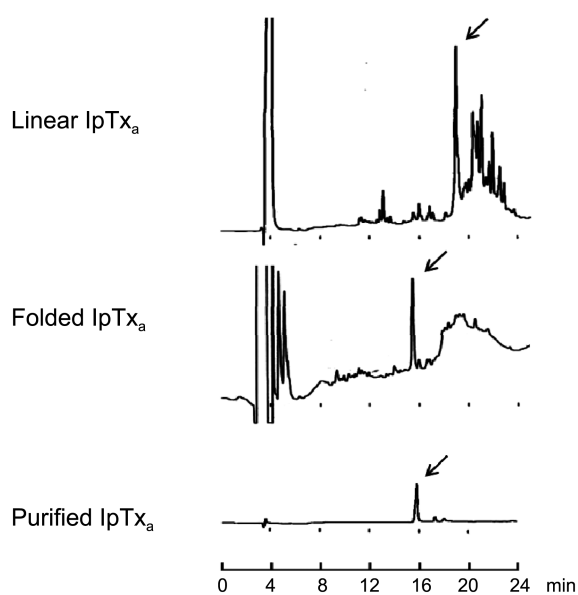


**Figure 2.** Reversed-phase HPLC profiles of oxidative folding and purification of IpTx<sub>a</sub>. Arrows indicate the product at each step.

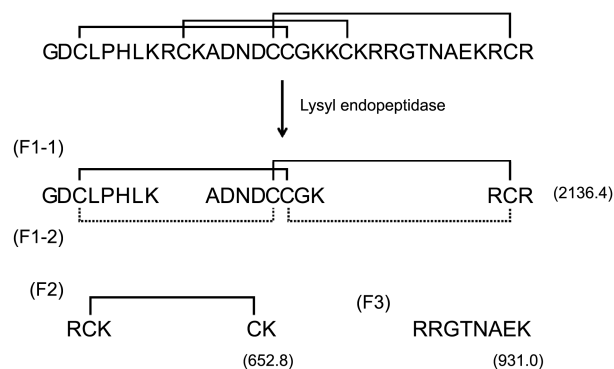


**Figure 3.** Scheme for identifying the intramolecular disulfide bonds in IpTx<sub>a</sub>. The peptide fragments (F1–F3) were released after peptidase treatment. The disulfide bonds of F1-1 and F1-2 are indicated as solid and dotted lines, respectively. The molecular weight of each fragment is shown in brackets.

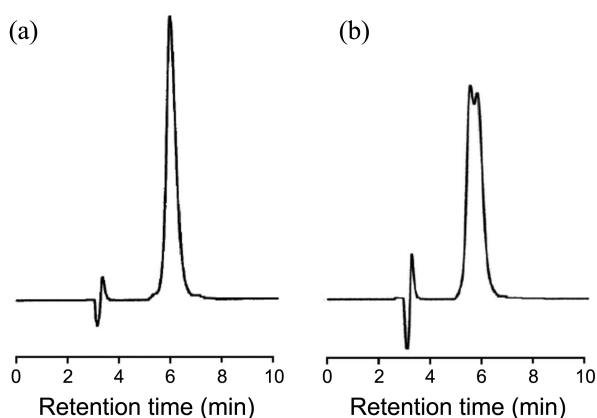


**Figure 4.** Comparison of two authentic fragments with enzymatic fragment from IpTx<sub>a</sub>. Co-injection of F1-1 (a) and F1-2 (b) with enzymatic fragment.

The identification of the enzymatic fragment by RP-HPLC and MALDI-TOF-MS measurements revealed that the fragment has two possible disulfide bond pairings that are Cys3-Cys17/Cys16-Cys31 or Cys3-Cys16/Cys17-Cys31 named F1-1 and F1-2, respectively (Figure 3). We could not detect the fragment of Cys10-Cys21 disulfide bond pairing on RP-HPLC. To select the alternatives of F1 fragments, we synthesized two authentic fragments that possessed two possible disulfide bond pairings. Co-injection of the enzymatic fragments from IpTx<sub>a</sub> with F1-1 or F1-2 clearly showed that the enzymatic fragment from IpTx<sub>a</sub> was identical with the F1-1 having the same retention time (Figure 4(a)). Therefore, we concluded that IpTx<sub>a</sub> has the disulfide bond connectivity as Cys3-Cys17, Cys10-Cys21 and Cys16-Cys31.

The CD spectrum of IpTx<sub>a</sub> shows two minima at around 205 nm and 280 nm and has the overall feature similar to those of  $\omega$ -conotoxin MVIIA and MVIIC (Figure 5). The three-dimensional structures of  $\omega$ -conotoxin MVIIA, MVIIC have been determined by two-dimensional NMR, revealing a triple-stranded antiparallel  $\beta$ -sheet stabilized by three disulfide bonds.<sup>7-9</sup> Although IpTx<sub>a</sub> and  $\omega$ -conotoxins exhibit high structural similarity, their biological functions are very different. IpTx<sub>a</sub> activates ligand-gated Ca<sup>2+</sup> channels. In contrast,  $\omega$ -conotoxins block various voltage-gated Ca<sup>2+</sup> channels. As we previously mentioned,<sup>6</sup> the surface properties of IpTx<sub>a</sub> and  $\omega$ -conotoxins are different so there is no cross activity between IpTx<sub>a</sub> and  $\omega$ -conotoxins, although they share the same disulfide bond framework. These results imply that the correct distribution of surface residues of the toxin molecule based on the correct disulfide bond connec-

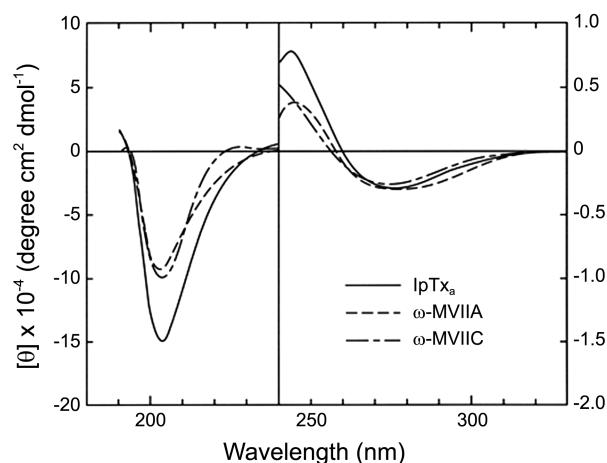


**Figure 5.** CD spectra of  $\omega$ -conotoxin MVIIA, MVIIC, and IpTx<sub>a</sub>.

tivity is critical to their biological activity.

**Acknowledgments.** This research was supported by “Leades Industry-university Cooperation” Project funded by the Ministry of Education, Science & Technology (MEST).

## References

- Creighton, T. E. *Methods Enzymol.* **1986**, *131*, 83.
- Richardson, J. S. *Adv. Protein Chem.* **1981**, *34*, 167.
- el-Hayek, R.; Lokuta, A. J.; Arevalo, C.; Valdivia, H. H. *J. Biol. Chem.* **1995**, *270*, 28696.
- Zamudio, F. Z.; Gurrola, G. B.; Arevalo, C.; Sreekumar, R.; Walker, J. W.; Valdivia, H. H.; Possani, L. D. *FEBS Lett.* **1997**, *405*, 385.
- Tripathy, A.; Resch, W.; Xu, L.; Valdivia, H. H.; Meissner, G. *J. Gen. Physiol.* **1998**, *111*, 679.
- Lee, C. W.; Lee, E. H.; Takeuchi, K.; Takahashi, H.; Shimada, I.; Sato, K.; Shin, S. Y.; Kim, D. H.; Kim, J. I. *Biochem. J.* **2004**, *377*, 385.
- Basus, V. J.; Nadasdi, L.; Ramachandran, J.; Miljanich, G. P. *FEBS Lett.* **1995**, *370*, 163.
- Farr-Jones, S.; Miljanich, G. P.; Nadasdi, L.; Ramachandran, J.; Basus, V. J. *J. Mol. Biol.* **1995**, *248*, 106.
- Kohno, T.; Kim, J. I.; Kobayashi, K.; Koder, Y.; Maeda, T.; Sato, K. *Biochemistry* **1995**, *34*, 10256.
- Lee, C. W.; Kim, S.; Roh, S. H.; Endoh, H.; Koder, Y.; Maeda, T.; Kohno, T.; Wang, J. M.; Swartz, K. J.; Kim, J. I. *Biochemistry* **2004**, *43*, 890.
- Kim, J. I.; Konishi, S.; Iwai, H.; Kohno, T.; Gouda, H.; Shimada, I.; Sato, K.; Arata, Y. *J. Mol. Biol.* **1995**, *250*, 659.
- Kubo, S.; Chino, N.; Kimura, T.; Sakakibara, S. *Biopolymers* **1996**, *38*, 733.
- Sasaki, T.; Feng, Z. P.; Scott, R.; Grigoriev, N.; Syed, N. I.; Fainzilber, M.; Sato, K. *Biochemistry* **1999**, *38*, 12876.